Energies **2015**, *8*, 1561-1583; doi:10.3390/en8031561

OPEN ACCESS

energies

ISSN 1996-1073

www.mdpi.com/journal/energies

Article

Deep Sediment-Sourced Methane Contribution to Shallow Sediment Organic Carbon: Atwater Valley, Texas-Louisiana Shelf, Gulf of Mexico

Richard B. Coffin [1,†,*], Christopher L. Osburn [2], Rebecca E. Plummer [3], Joseph P. Smith [4], Paula S. Rose [1,†] and Kenneth S. Grabowski [1]

[1] Naval Research Laboratory, Washington, DC 20735, USA; E-Mails: paula.rose@tamucc.edu (P.S.R.); kenneth.grabowski@nrl.navy.mil (K.S.G.)

[2] Marine, Earth, and Atmospheric Sciences, North Carolina State University, Raleigh, NC 27695, USA; E-Mail: closburn@ncsu.edu

[3] Department of Geology, University of Maryland, College Park, MD 20742, USA; E-Mail: rplummer@umd.edu

[4] Oceanography Department, US Naval Academy, Annapolis, MD 21402, USA; E-Mail: jpsmith@usna.edu

† Current Address: Department of Physical and Environmental Sciences, Texas A&M University—Corpus Christi, Corpus Christi, TX 78412, USA.

* Author to whom correspondence should be addressed; E-Mail: richard.coffin@tamucc.edu; Tel.: +1-361-825-2456.

Academic Editor: Enrico Sciubba

Received: 23 August 2014 / Accepted: 11 February 2015 / Published: 18 February 2015

Abstract: Coastal methane hydrate deposits are globally abundant. There is a need to understand the deep sediment sourced methane energy contribution to shallow sediment carbon relative to terrestrial sources and phytoplankton. Shallow sediment and porewater samples were collected from Atwater Valley, Texas-Louisiana Shelf, Gulf of Mexico near a seafloor mound feature identified in geophysical surveys as an elevated bottom seismic reflection. Geochemical data revealed off-mound methane diffusion and active fluid advection on-mound. Gas composition (average methane/ethane ratio ~11,000) and isotope ratios of methane on the mound (average $\delta^{13}C_{CH4(g)}$ = −71.2‰; $\Delta^{14}C_{CH4(g)}$ = −961‰) indicate a deep sediment, microbial source. Depleted sediment organic carbon values on mound ($\delta^{13}C_{SOC}$ = −25.8‰; $\Delta^{14}C_{SOC}$ = −930‰) relative to off-mound ($\delta^{13}C_{SOC}$ = −22.5‰;

$\Delta^{14}C_{SOC}$ = −629‰) suggest deep sourced ancient carbon is incorporated into shallow sediment organic matter. Porewater and sediment data indicate inorganic carbon fixed during anaerobic oxidation of methane is a dominant contributor to on-mound shallow sediment organic carbon cycling. A simple stable carbon isotope mass balance suggests carbon fixation of dissolved inorganic carbon (DIC) associated with anaerobic oxidation of hydrate-sourced CH_4 contributes up to 85% of shallow sediment organic carbon.

Keywords: methane; advection; geochemistry; carbon isotopes; sediment carbon

1. Introduction

Sediment organic carbon (SOC) composition and provenance have been extensively studied in the Gulf of Mexico (GoM). Generally, inputs of terrestrially-derived organic carbon (OC) dominate near shore sediments and decrease with distance offshore [1–5]. Terrestrial-derived OC in surficial sediments of the GoM shifts from C3 plant material near shore to highly degraded, soil-derived material offshore [1–3]. Surface sediments on the slope (365–2270 m water depth) have $\Delta^{14}C$ values between −309.1‰ and −228.6‰ corresponding to 64% to 78% modern carbon [3]. Mayer *et al.* [4] calculated that surficial SOC on the slope is 41% to 46% of marine origin. Carbon isotope signatures typical for marine phytoplankton have been measured in surface sediments at water column depths from 74 to 2250 m (mean $\delta^{13}C$ value = −20.8‰; [6]). In the same study, depleted ($\delta^{13}C$ = −24.1‰) sedimentary organic matter was observed at a cold seep site (688 m water depth) that suggested a contribution of seep hydrocarbons to sediment organic matter.

Methane hydrate deposits are abundant in deep sediments along the Texas-Louisiana Shelf [7,8]. Hydrate-sourced CH_4 may contribute to the sediment OC pool and should be considered in investigations of carbon cycling and regional carbon mass balance calculations. During anaerobic oxidation of methane (AOM), bacteria utilize seawater-sourced sulfate (SO_4^{2-}) as a terminal electron acceptor to oxidize methane as an energy source, and produce sulfide (H_2S) and dissolved inorganic carbon (DIC) in the process [9,10]. During this oxidation porewater DIC sourced from downward seawater diffusion, upward deep system advection or diffusion, and AOM is incorporated into microbial biomass [11–14]. This is a contrast to aerobic CH_4 assimilation, where methane-derived carbon is directly incorporated into microbial biomass [15]. Deep sediment hydrocarbons, including CH_4, have been shown to contribute to carbon cycling in shallow sediments and the water column [16–21]. However, the indirect contribution of hydrate-sourced CH_4 to shallow sediment carbon pools through AOM and subsequent carbon dioxide (CO_2) fixation has not been thoroughly evaluated.

Shallow sediment CH_4 in Atwater Valley, Gulf of Mexico has been shown to be dominated by biogenic gas from deep sediments [17]. In this study, two sites in Atwater Valley were contrasted: A sediment mound with active fluid advection and high vertical CH_4 flux and an off-mound site exhibiting steady-state CH_4 diffusion [22,23]. Gas speciation and $\delta^{13}C$ values at both sites indicate that the shallow sediment gas is primarily biogenic-sourced CH_4, absent of higher molecular weight gases [22]. In this study a carbon budget is constructed for each site using hydrocarbon gas concentrations and stable carbon isotope ($\delta^{13}C$) and radiocarbon isotope ($\Delta^{14}C$) signatures of the

organic and inorganic carbon pools in solid phase sediment and pore water. The hypothesis is that dissolved inorganic carbon (DIC) assimilated during AOM is a dominant contributor to on-mound shallow sediment organic carbon cycling.

2. Materials and Methods

2.1. Study Location

Atwater Valley is a shallow trough in the Mississippi Canyon, Gulf of Mexico (Figure 1a). This underwater trough is part of the Mississippi Fan Fold-belt with sediment features including basinward-verging anticlines and underlain southern verging thrust faults across a 300 km long and 50 km wide region. Fold strata were formed during Late Jurassic to Miocene geologic periods resulting in formation of substantial salt tongues and sheets [24]. Canyon fill through the gas hydrate stability zone (HSZ) is comprised of fine-grained sediments, mostly interbedded debris flows and hemipelagic sediments overlain by a fine Holocene pelagic drape [25]. The area is characterized by seafloor mounds and basins formed through vertical advection of hydrocarbons, minerals, and CH_4-rich fluids [26].

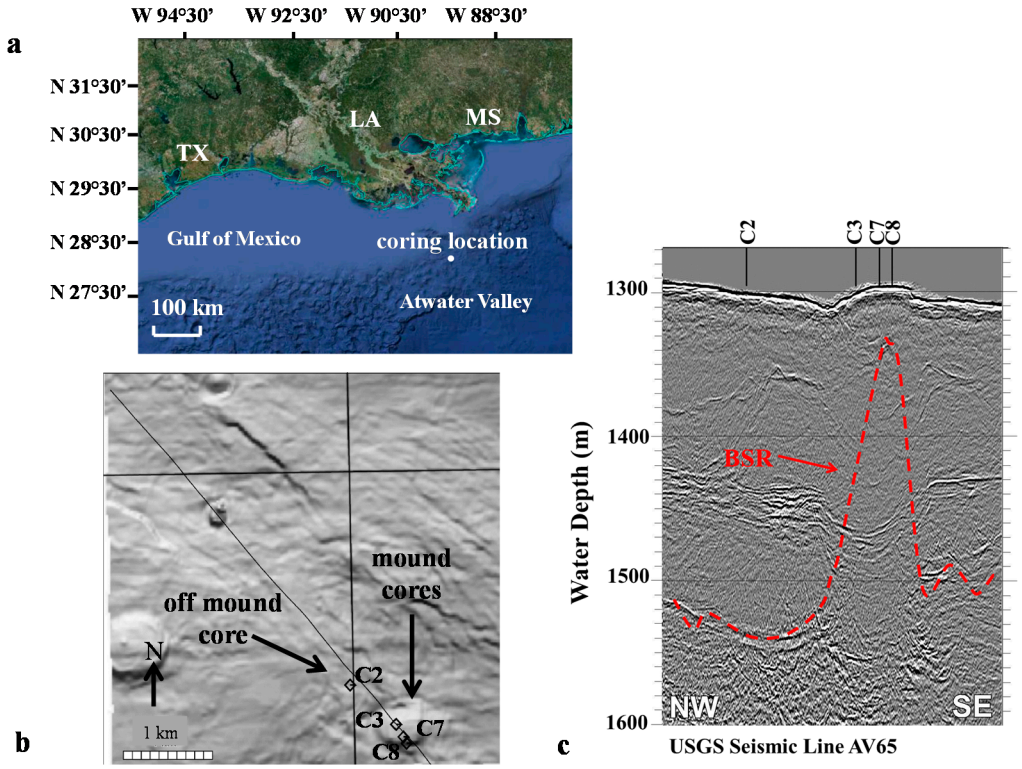

Figure 1. (**a**) Atwater Valley, Gulf of Mexico, Texas-Louisiana Shelf coring location (provided by Google Earth); (**b**) Sediment floor contours through the sample region, with sites on- (cores 3,7,8) and off-mound (core 2), the solid line represents the seismic data transect through the coring locations; (**c**) Core sites selected for this study were over a strong sediment bottom reflection (BSR) off-mound and on the mound observed with an elevated BSR and vertical seismic blanking above the BSR mound.

A 4 m high seafloor mound, at a water column depth between 1296 and 1300 m, was chosen as a study site based on previous seismic and geochemical studies conducted in May 2004 [22,23,27]

(Table 1). A key mound feature (Figure 1b) is a shallowing bell-shaped bottom simulating reflection (BSR) that raises approximately 200 m relative to off-mound BSR at 240 mbsf (Figure 1c, Table 1). At this location, heat flow elevates from a background signature off-mound of 40 to 160 $mW \cdot m^{-2}$ on-mound (Table 1). These geophysical conditions on mound were interpreted to be a thermal perturbation to the HSZ base, creating vertical fluid fluxes [23].

Porewater chloride (Cl^-) concentrations on-mound averaged 934 ± 74 mM, well above the seawater background, indicating active vertical advection of higher salinity porewaters (Table 1) and a rise in the BSR (Figure 1c). This interpretation is supported with the observation of Late Jurassic to Miocene salt tongues and salt diapirism in this region that would reduce deep sediment hydrate stability [24]. An advective CH_4 flux of 3250 $mM \cdot m^{-2} \cdot year^{-1}$ was estimated on the mound (Table 1). In contrast, 750 m off-mound (Figure 1b) a moderate diffusive CH4 flux of 20.6 $mM \cdot m^{-2} \cdot year^{-1}$ was observed (Table 1). Off-mound, sediment porewater SO_4^{2-} concentrations were observed to decrease linearly from near seawater values at the sediment-water interface to below detection limits at 410 centimeters below the sea floor (cmbsf). Below 410 cmbsf, sediment headspace methane concentrations increased linearly, indicating a sulfate methane-transition (SMT) supported by the anaerobic oxidation of methane (AOM). Vertical fluid advection limited downward SO_4^{2-} diffusion on-mound (Table 1).

Table 1. Review of previously published data for core sites on- and off-mound. Where data is general for the mound and not located at specific stations it is listed under C7.

Parameter	Cores				
	Off Mound	Mound			
	C2	C7	C3	C8	Ref.
Latitude	27°56′26.644	27°56′26.644	27°56′26.644	27°56′26.644	[27]
Longitude	89°16′49.696	89°16′49.696	89°16′49.696	89°16′49.696	[27]
Water Column Depth (m)	1300	1296	1301	1296	[27]
Core Pentetration (cmbsf)	470	867	515	370	[27]
SMT (cmbsf)	410	no SMT	no SMT	59	[22]
Methane Flux (mM CH_4 $m^{-2} \cdot year^{-1}$)	20	3250	ND	167	[22]
Average Cl^- (mM)	551 ± 6	934 ± 44	911 ± 79	770 ± 102	[22]
Heat Flow ($mW \cdot m^{-2}$)	40	160	-	-	[22]
BSR depth (mbsf)	240	40	-	-	[23]

Close proximity in spatial variation of downward SO_4^{2-} diffusion and inferred vertical CH_4 flux observed in previous studies on this mound makes it a unique study site to investigate CH_4 contribution to shallow sediment carbon cycling [22]. Porewater and sediment inorganic and organic carbon concentration and carbon isotope ratio data from an off-mound core (C2) are compared to an on-mound core (C7). Results from two additional sediment mound cores (C3 and C8) located near C7 are used to provide additional data for interpretation of CH_4 contribution to sediment carbon pools (Table 1).

2.2. Sediment Core Collection and Processing

Piston cores C7, C3, and C8 were collected on-mound (water depth = 1296 m) and C2 was collected off-mound (water depth = 1300 m, Figure 1b,c). For on-mound cores C7 was located near the

center, while C3 and C8 were near the mound edge, 150 and 70 m, respectively, from C7. Sediment cores were collected and processed shipboard as described in Coffin *et al.* [22]. Briefly, sediment cores were obtained using a 10 m piston coring system with 2.75 polycarbonate core liners. Cores ranged in length from ~300 to 800 cm and were processed immediately onboard the ship.

Core liners were inspected for gas pockets and gas expansion voids. At void spaces, the liner was drilled and gas sampled with a 60 mL polypropylene syringe fitted with a modified 3-way stopcock. Gas samples were then transferred to 30 mL pre-evacuated, glass serum vials fitted with a gastight stopper and aluminum seal. Subsequently, sediment plugs were collected from regular intervals along the core using a 3 mL polypropylene syringe with the tip cut off, transferred to pre-weighed 20 mL serum vials, and capped with gastight stoppers and aluminum seals to determine sediment headspace light hydrocarbon concentrations; (CH_4 through C_3H_8) as well as $\delta^{13}C_{CH4(g)}$ ratios.

For additional sampling, core liners were removed and cut in 10 cm sections within an interval of 25–45 cm. Wet sediment from each section was frozen in snap-tight Petri-dishes for laboratory measurements of sediment porosity and percent organic carbon. Porewater pressed from sediment using 70 mL Reeburgh-style PVC press containers pressurized to 400 KPa (60 psi) by a low-pressure air on a latex sheet between core sections and press gas inflow was collected into 60-mL polypropylene syringes [28]. Porewater was filtered from syringes through ashed Whatman GF-F filters into ashed 20 mL vials and subsequently distributed into appropriate vials for each analysis; 2 mL in a 5 mL glass serum vial for [DIC]; 1 mL in a 2 mL glass serum vial for $\delta^{13}C_{DIC}$, and; 2 mL in a 5 mL glass screw-top vial for dissolved organic carbon concentration [DOC] and $\delta^{13}C_{DOC}$. Pressed sediment for inorganic and organic carbon concentration and isotope analyses was wrapped in ashed aluminum foil, sealed in Whirlpack bags, and stored frozen at −20 °C for analyses at the land-based laboratory.

2.3. Shipboard Analyses

To extract volatile hydrocarbons from sediment into vial headspace for gas analysis, 3 mL of nitrogen sparged, deionized water was injected through the septum of the serum vial and vial was shaken for 3 min. After this extraction, the headspace sample was removed from the vial and injected into a sampling loop on a Shimadzu GC-14A gas chromatograph-flame ionization detector (GC-FID) with a Hayesep-Q packed column (Alltech, Deerfield, IL, USA) to measure CH_4, ethane (C_2H_6), and propane (C_3H_8) concentrations. Sediment CH_4 concentrations were corrected for atmospheric background in the vials (95% extraction efficiency was assumed). Core gas pocket C_1-C_3 alkane concentrations were also measured using the GC-FID. Analytical precision was within 0.1 mM, based on replicate analyses. The limit of detection for methane was 0.009 mM and where concentrations were lower data are presented as 0.0 mM.

Porewater DIC concentrations were determined using a UIC CO_2 coulometer (UIC, Inc., Joliet, IL, USA) standardized to a certified seawater reference material (University of California, San Diego, CA, USA). Replicate variability was less than 0.15 mM.

2.4. Post-Cruise Laboratory Analyses

Sediment total carbon and OC (%TC, %SOC) concentrations and $\delta^{13}C$ values were determined on a Fisons EA 1108 C/H/N analyzer in line with a Thermo Electron Delta Plus XP Isotope Ratio Mass

Spectrometer (IRMS) interface via a Conflo II (Thermo Scientific, Waltham, MA, USA). Pressed sediment was dried at 80 °C, ground with a mortar and pestle, then 15 to 20 mg of sediment was weighed in tin capsules for TC analysis. For SOC analysis, sub-samples were weighed in silver capsules, treated with an excess of 10% HCl and dried in an oven at 70 °C overnight to remove inorganic carbon. Sediment inorganic carbon (%$CaCO_3$) concentrations were determined from the difference between TC and SOC. A concentration calibration curve for carbon concentration analysis was generated daily by analyzing an acetanilide standard. For sediment $\delta^{13}C_{SOC}$ values, IAEA-C8 (oxalic acid), IAEA-CH-6 (sucrose) and USGS 40 (l-glutamic acid) were used as calibration standards. Acetanilide standards (USGS-40 and IAEA-C8) were also used as check standards during analysis. All $\delta^{13}C$ data presented in this work are in per mil units (‰) and referenced to the Vienna Pee Dee Belemnite (VPDB) scale. Errors were based on triplicate runs. Error for % SOC was within ±0.03%C, %$CaCO_3$ varied by less 0.2%, and $\delta^{13}C_{SOC}$ varied by less than 0.2‰.

Sediment $\delta^{13}C_{CaCO3}$, pore water $\delta^{13}C_{DIC}$, and gas pocket and sediment $\delta^{13}C_{CH4}$ ratios were determined using a Thermo Electron Trace GC equipped with a Varian Porapak-Q column and GC-CIII combustion interface in-line with the Delta Plus XP IRMS (Thermo Scientific, Waltham, MA, USA) [22]. For $\delta^{13}C_{CaCO3}$ analysis, 250 mg of sediment in a serum vial was treated with 2 mL of 10% HCl. For $\delta^{13}C_{DIC}$ analysis, 2 mL porewater samples were treated with 200 μL of 85% H_3PO_4. In both cases, CO_2 was extracted from the vial headspace and injected into the GC via a split/splitless inlet in split mode. All $\delta^{13}C_{CaCO3}$ and $\delta^{13}C_{DIC}$ values were normalized through analysis of CO_2 and C_1-C_5 alkanes in NIST RM 8560 (natural gas, petroleum origin). Samples for $\delta^{13}C_{CH4}$ analysis were introduced via an in-line cryogenic focusing system according to the method of Plummer *et al.* [29]. A separate $\delta^{13}C$ normalization curve was generated for C_1-C_4 alkanes and used to normalize $\delta^{13}C_{CH4}$ data. Replicate $\delta^{13}C_{CaCO3}$ values varied by less than 0.2‰, δ^{13}CDIC by less than 0.5‰, and $\delta^{13}CCH_4$ by less than 1.0‰.

Porewater DOC was measured on an OI Analytical 1010 total organic carbon analyzer (OI Analytical, College Station, TX, USA) using a heated persulfate oxidation method modified for seawater analyses [30]. The samples were kept frozen until ready for analysis, then acidified and nitrogen sparged in the lab prior to analysis to remove DIC. The total organic carbon analyzer was interfaced with the Delta Plus XP IRMS. A DOC calibration curve was generated using standards of potassium hydrogen phthalate. Measured $\delta^{13}C_{DOC}$ values were normalized to the VPDB scale by analyzing solutions of IAEA-CH-6 (= −10.449 ± 0.033‰) and USGS 40 (−26.389 ± 0.042) standards. Using triplicate analyses, DOC concentrations varied by less than 0.02 mM, and $\delta^{13}C_{DOC}$ varied by less than 0.2‰.

2.5. Radiocarbon Isotope Analysis

Graphite sample preparation for $\Delta^{14}C$ analysis of CH_4 and SOC are described in detail by Pohlman *et al.* [31]. Targets were prepared in the U.S. Naval Research Laboratory (NRL) Graphite Lab. Targets were then analyzed at the NRL accelerator mass spectrometer (AMS) facility using an AMS equipped with a high intensity cesium sputter source for ^{14}C analysis [32]. Data analysis was according to standard procedures described in Tumey *et al.* [33]. Samples were measured against OX II standards and blanks distributed throughout loadings of the sample wheel. On average, each wheel contained 2 AMS blanks for tuning the accelerator, three processing blanks appropriate for the samples on the wheel, and 7 OX II standards. $\delta^{13}C$ results were obtained from GC-IRMS analysis of the samples.

These values were used to calculate the δC fractionation correction for each sample. The $\Delta^{14}C$ data were calculated as:

$$\Delta^{14}C = \left[\frac{R_{sn}}{R_{abs}} - 1\right] \times 1000 \quad (‰) \tag{1}$$

where R is $^{14}C/^{13}C$ or $^{14}C/^{12}C$, R_{sn} represents the sample with normalization to a standardized $\delta^{13}C$ and R_{abs} represents oxalic acid standards normalized to a $\delta^{13}C$ standard and the standardized atmospheric ^{14}C level in 1950 [34–36]. To compare the influence of C cycling with aging of deposited sediment, $\Delta^{14}C$ was converted to conventional radiocarbon age (CRA) where:

$$t = -8033\left[\ln\left(\frac{\Delta^{14}C}{1000} + 1\right) + \lambda\left(y - 1950\right)\right] \tag{2}$$

In this equation, t is the CRA in years before present (1950), using the Libby half-life for ^{14}C ($t_{1/2}$ = 5568 years). To obtain actual calendar years, a standardized conversion was applied. The $\Delta^{14}C$ term is the value obtained after the ^{13}C correction is applied, λ is the ^{14}C constant (1/8267 years), and y is the year of measurement. Thus, for $\Delta^{14}C$ of 0, t would be 0 for a measurement performed in 1950 and 1955 for 2007, when the measurement was performed [33].

2.6. $\delta^{13}C$ Data Interpretation

The relative contribution of CH_4 to the shallow sediment carbon pools on-mound with a high advection and off-mound with a moderate diffusion assumes microbial assimilation of DIC during AOM [37]. Methane contribution at these different flux rates is summarized at specific core depths or averages through the sulfate methane transition zone. Accounting for isotope fractionation during assimilation, DIC contribution to organic carbon pools is estimated using a simple, two end-member isotope mass balance [38]:

$$R_x = R_{\mathrm{PD}}C_{\mathrm{PD}} + R_{\mathrm{DIC}}C_{\mathrm{DIC}} \tag{2}$$

where R_x represents $\delta^{13}C$ of SOC or DOC and the isotopic composition of marine phytodetritus (PD) and DIC are represented by R_{PD} and R_{DIC}, respectively. The variables C_{PD} and C_{DIC} represent the corresponding fractional contributions of marine PD and DIC such that:

$$C_{\mathrm{PD}} + C_{\mathrm{DIC}} = 1 \tag{3}$$

The percent contribution of DIC to each carbon pool (%X) can then be derived from Equations (3) and (4):

$$\%X = \frac{R_x - R_{\mathrm{PD}}}{R_S - R_{\mathrm{PD}}} \times 100 \tag{4}$$

where R_s represents the isotopic composition of DIC. Consideration of isotope fractionation during DIC assimilation is presented in the Discussion.

3. Results

Results focus on a comparison of off-mound (C2) and on-mound (C7) CH_4 contribution to organic carbon in gas, porewater and sediment samples. Core C3 provides supplementary data for assessing the

on-mound CH_4 flux and cycling. Core C8, located near the edge of the mound, shown to have active vertical CH_4 diffusion [22], is also used in data interpretation.

3.1. Radiocarbon

The $\Delta^{14}C_{CH4(g)}$ values measured in gas pockets of near-mound cores C3 and C8 taken close to the primary mound core are presented in Figure 2 and Table 2. The gas pockets in core C8 were slightly enriched in ^{14}C relative to gas pockets in core C3. On-mound SOC in core C7 was substantially more ^{14}C-depleted than SOC in off-mound core C2 (Figure 2). In each core, the shallowest sediments had a more modern radiocarbon age, however, there was a large difference in the $\Delta^{14}C_{SOC}$ data between the cores. To estimate a change in apparent sediment age caused by the presence of CH_4, a sedimentation rate of 0.037 ± 0.022 cm·year^{-1} [3] and natural radiocarbon decay starting at shallow sediment off-mound $\Delta^{14}C$ value (−283‰) was applied to data to construct a conservative age line (Figure 3). CRA in off-mound and on-mound SOC did not conform to the predicted conservative age line. In the shallow section of the off-mound core, carbon age was older than predicted aging line down to approximately 300 cm and was younger below 300 cm. On-mound sediment CRA was older than the age line through the core.

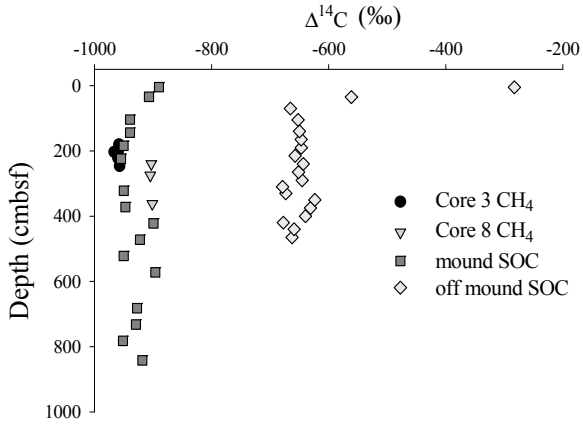

Figure 2. $\Delta^{14}C_{CH4}$ of free gas and SOC at on-mound and off-mound sites.

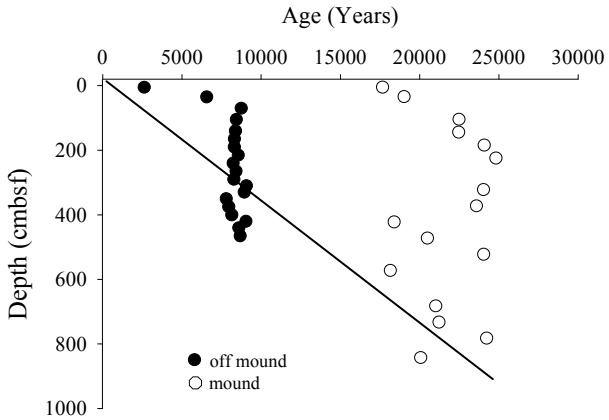

Figure 3. Conventional radiocarbon age of SOC for cores taken off- and on-mound. The conservative aging line shown was calculated using estimates of annual sedimentation rate for this region.

3.2. Solid Phase Sediment Profiles

An overview of all carbon pool concentration and $\delta^{13}C$ data is presented in Table 2. A complete data set is available in Supplementary. Sediment OC concentrations were higher in off-mound C2 core than on-mound C7 core (Figure 4a, Table 2). On-mound $\delta^{13}C_{SOC}$ values showed strong ^{13}C-depletion near the seawater interface (SWI, Figure 4b). Off-mound SOC was more ^{13}C-enriched with higher values near surface above the SMT of 410 cmbsf (Figure 4b, Table 1). Profiles of $CaCO_3$ (Figure 4c) and $\delta^{13}C_{CaCO3}$ (Figure 4d) also were substantially different when compared on- and off-mound. $CaCO_3$ as a percentage of total sediment mass was substantially higher on-mound (average = 11.4 ± 1.1%, n = 16) than off-mound (average = 4.1 ± 3.0%, n = 19). Sediment $\delta^{13}C_{CaCO3}$ values were generally ^{13}C-enriched on-mound (average = −2.7 ± 2.8‰, n = 16) relative to off-mound (average = −4.5 ± 2.4‰, n = 19). However, at the SWI, on-mound $\delta^{13}C_{CaCO3}$ value was ^{13}C-depleted while off-mound $\delta^{13}C_{CaCO3}$ was ^{13}C-enriched.

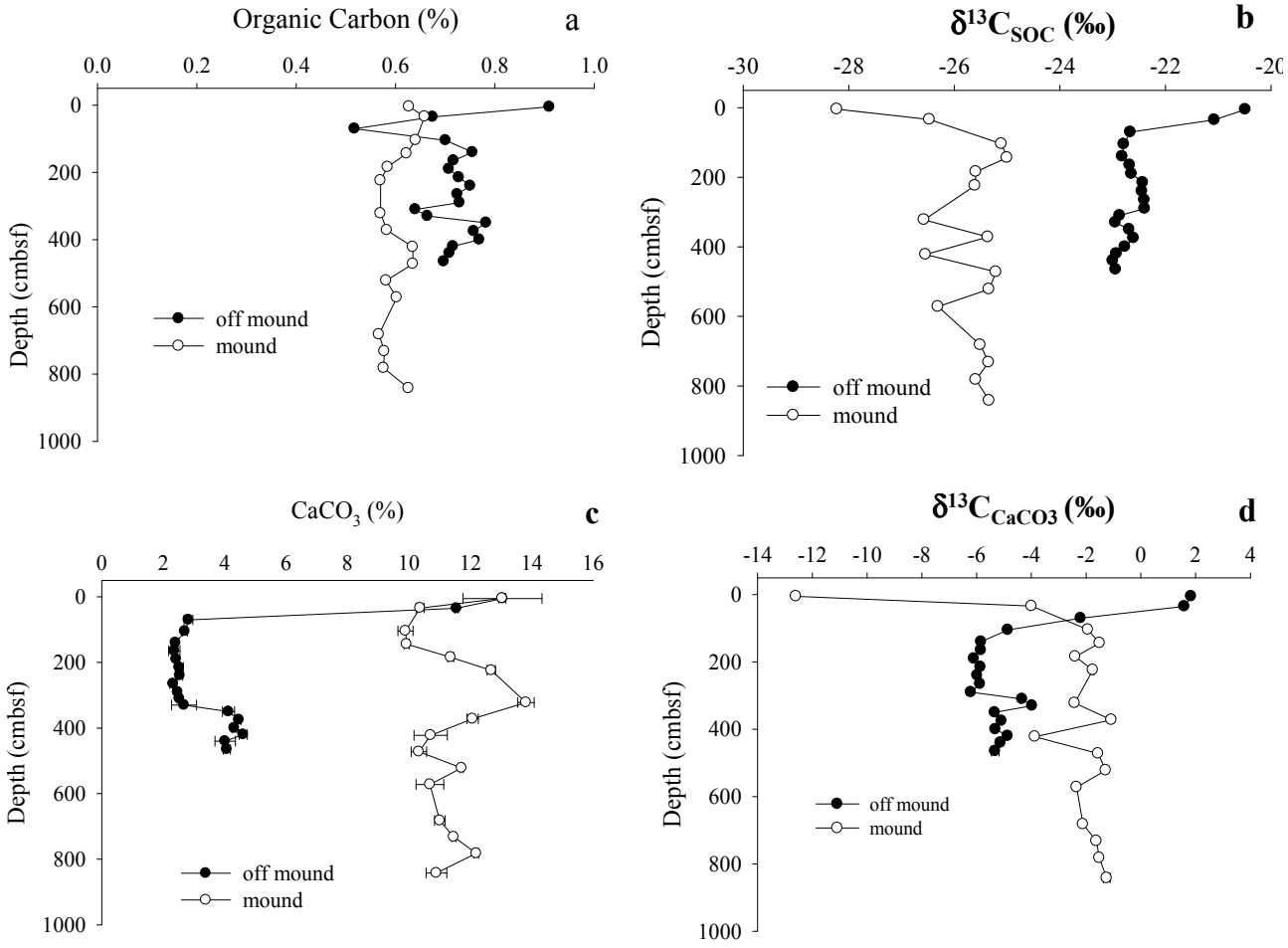

Figure 4. Sediment profiles at on-mound and off-mound sites: (**a**) Percent sediment organic carbon (SOC); (**b**) $\delta^{13}C_{SOC}$; (**c**) percent $CaCO_3$; and (**d**) $\delta^{13}C_{CaCO_3}$.

Table 2. Summary of C pool concentrations and $\delta^{13}C$, with minimum, maximum and average values for each core. The full data set for each core is available in Supplementary.

Core ID	Gas		Porewater						Sediment				
	$\delta^{13}C_{CH4}$	$\Delta^{14}C_{CH4}$	CH_4 (mM)	$\delta^{13}C_{CH4}$	DIC (mM)	$\delta^{13}C_{DIC}$	DOC (mM)	$\delta^{13}C_{DOC}$	% SOC	$\delta^{13}C_{SOC}$	$\Delta^{14}C_{SOC}$	% $CaCO_3$	$\delta^{13}C_{TIC}$
C2													
Min	ND	ND	LOD	−86.9	2.8	−47.1	0.82	−26.2	0.91	−23	−679	2.4	−6.1
Max	ND	ND	12.5	−48.8	20	−9.4	3.64	−20.1	0.64	−20.5	−283	13.04	1.8
AVG ± SD	ND	ND	5.3 ± 5.5	−74.1 ±11.5	10.2 ± 5.3	−27.6 ± 11.5	2.06 ± 1.18	−23.9 ± 1.5	0.72 ± 0.07	−22.5 ± 0.6	−629 ± 88	4.4 ± 3.2	−4.6 ± 2.4
C3													
Min	−72.5	−963	0.1	−75.4	6.7	−42.9	ND	ND	ND	ND	ND	ND	ND
Max	−72	−957	7.9	−72.8	13.6	3.7	ND	ND	ND	ND	ND	ND	ND
AVG ± SD	−72.3 ± 0.2	−960 ± 3	4.2 ± 1.8	−73.7 ± 0.9	9.7 ± 2.3	−3.0 ± 12.6	ND	ND	ND	ND	ND	ND	ND
C7													
Min	−71.4	ND	3.3	−82	5.6	−48.1	2.05	−27.6	0.57	−28.2	−951	9.89	−12.6
Max	−71.2	ND	10.6	−69	12.1	4.6	3.92	−24.8	0.66	−25	−890	13.04	−1.1
AVG ± SD	−71.3 ± 0.3	ND	6.2 ± 1.8	−70.4 ± 3.3	7.3 ± 1.6	−3.4 ± 14.4	3.55 ± 0.42	−25.6 ± 0.8	0.60 ± 0.03	−25.8 ± 0.8	−929 ± 22	11.4 ± 1.1	−2.7 ± 2.8
C8													
Min	−72.3	−905	0.0	−85.2	5.5	−44.3	ND	ND	ND	ND	ND	ND	ND
Max	−65.8	−901	13.0	−71.5	13.8	6.7	ND	ND	ND	ND	ND	ND	ND
AVG ± SD	−69.7 ± 3.4	−903 ± 2	5.64 ± 3.62	−76.6 ± 3.9	10.6 ± 2.0	−15.0 ± 21.7	ND	ND	ND	ND	ND	ND	ND

3.3. Gas Sources and Sediment and Porewater Carbon Profiles

Through the discussion we assume that shallow CH_4 originates from deep sediment CH_4 fluxes; deep CH_4 is based on on-mound core liner gas pocket data. Assuming void gas from core liner pockets is a deeper source is supported with depleted $\Delta^{14}C_{CH4}$ data (see Section 3.1. Radiocarbon), coupled with observation of elevated Cl^- profiles (Table 1) indicating deep vertical advection to the shallow system. Further support for this interpretation is presented below with on-mound porewater DIC data. This $\delta^{13}C_{CH4}$ value is compared to sediment headspace methane ($CH_4(g)$) to assess shallow sediment cycling (Table 2). Measured $\delta^{13}C_{CH4(g)}$ values from on-mound core C7 and near-mound core C3 showed little variation within and between cores. Variation of $\delta^{13}C_{CH4(g)}$ was greater and moderately depleted in ^{13}C in near-mound core C8. For all cores with gas pockets in which ethane was detected, the C_1/C_2 ratios were high ([27]; average 11,000, n = 13). As a note, all CH_4 concentrations shown in Table 2 are relative (headspace) measurements and underestimate actual sediment methane concentrations as a result of pressure changes during core retrieval from the ocean floor resulting in degassing [21].

Off-mound (C2) CH_4 concentrations were highest below the apparent SMT at 410 cmbsf (Table 2) and near the limit of detection above the SMT (Figure 5a). On-mound CH_4 concentrations were higher in shallow sediments (C3, C7, and C8), relative to off-mound, and showed a general decrease toward the sediment-water interface (SWI). On-mound sediment $\delta^{13}C_{CH4}$ was relatively uniform through the profile except for ^{13}C depletion at the SWI (Figure 5b). Mound core C3 had a similar profile with moderate ^{13}C depletion through the profile. More variation was observed in on-mound core C8, with ^{13}C-depletion observed at 50 cmbsf (Figure 5b). Off-mound sediment CH_4 was ^{13}C-enriched in shallow sediments up to 260 cmbsf and was depleted deeper than 300 cmbsf (Figure 5b). Off-mound $\delta^{13}C_{CH4}$ data are not presented above 260 cmbsf because CH_4 concentrations were below the limits of detection for carbon isotope analyses.

On-mound (C7) porewater DIC concentrations increased from the SWI to 34 cmbsf, and subsequently decreased towards the core base (Figure 6a). Off-mound (C2) porewater DIC concentrations gradually increased from a SWI minimum to a maximum at 350 cmbsf and then declined rapidly toward the core base. On-mound, $\delta^{13}C_{DIC}$ values decreased to most depleted ^{13}C value at 34 cmbsf where concentration increased; below this point $\delta^{13}C_{DIC}$ values increased and remained uniform (Figure 6b). Off-mound $\delta^{13}C_{DIC}$ values showed a similar patter with the minimum value at 330 cmbsf.

While on-mound and off-mound porewater DOC concentration ranges were similar, notable differences in vertical profiles were observed (Figure 7a). Off-mound DOC concentrations in porewaters were lowest in near surface sediments and generally increased with depth. On-mound porewater DOC concentrations were relatively consistent throughout the profile, except for a low value near surface. On-mound porewater $\delta^{13}C_{DOC}$ values showed little variation, however, porewater DOC was substantially ^{13}C-depleted throughout the core with a minimum value at 34 cmbsf (Figure 7b). In contrast, off-mound porewater $\delta^{13}C_{DOC}$ values varied substantially and were generally ^{13}C-enriched; $\delta^{13}C_{DOC}$ values were elevated in samples taken less than 100 cmbsf and depleted below 100 cmbsf (Figure 7b).

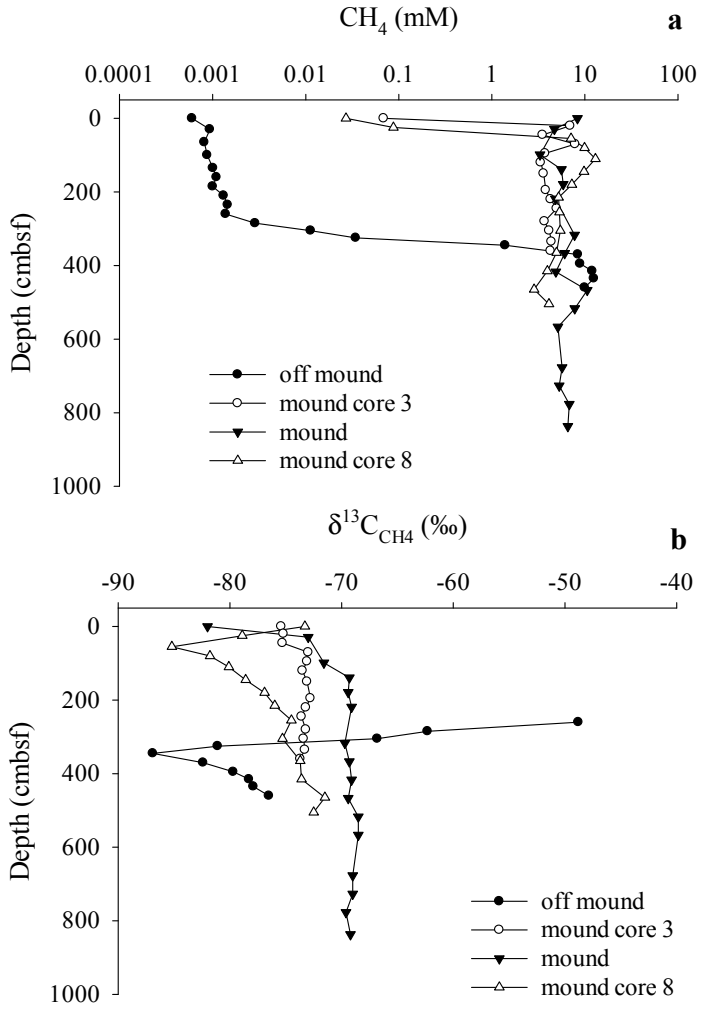

Figure 5. (**a**) Sediment CH_4 concentrations; and (**b**) $\delta^{13}C_{CH_4}$ values measured for on-mound (C7) and off-mound (C2) core locations. On-mound cores include cores 3 and 8 that are used for estimating the C isotope values for source CH_4 and interpretation of mound C cycling.

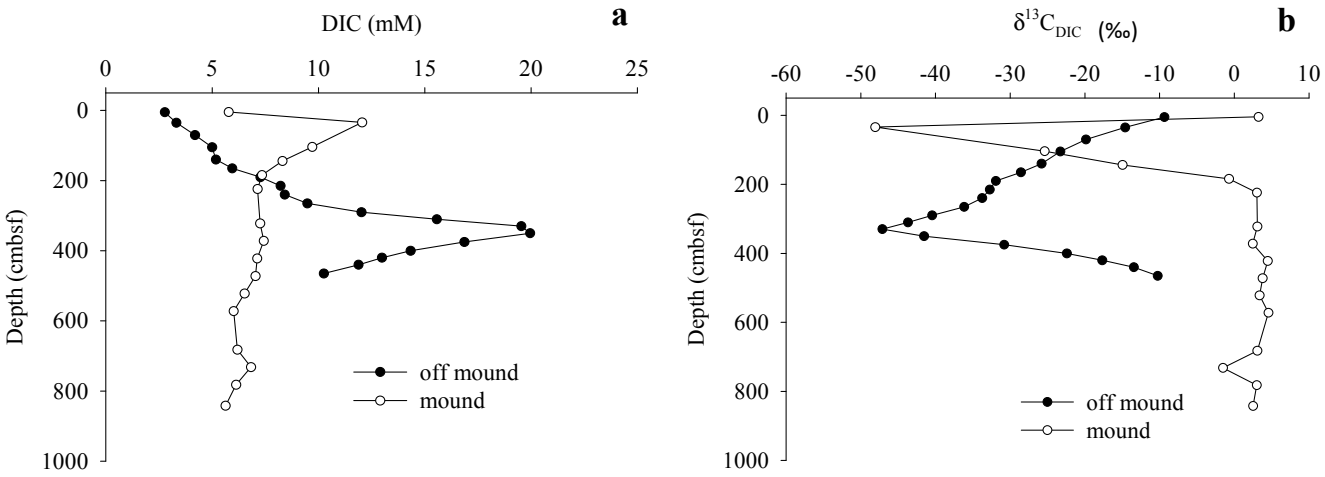

Figure 6. (**a**) Sediment pore water dissolved inorganic carbon (DIC) concentrations; and (**b**) $\delta^{13}C_{DIC}$ values measured on-mound and off-mound.

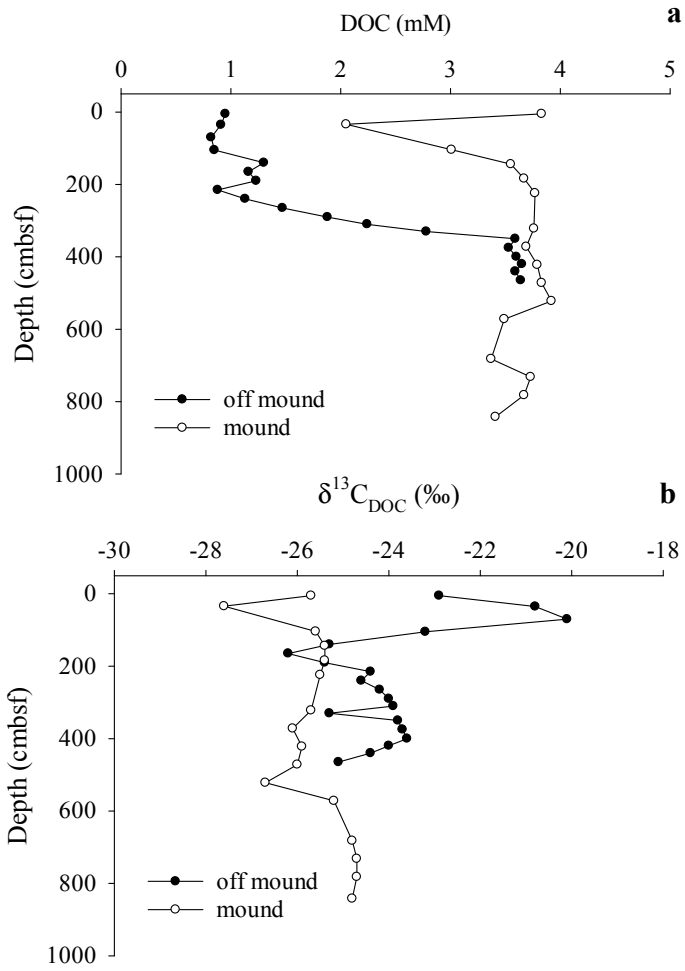

Figure 7. (**a**) Vertical profiles of sediment pore water dissolved organic carbon (DOC) concentrations compared on-mound and off-mound; and (**b**) Vertical profiles of $\delta^{13}C_{DOC}$ values measured on-mound and off-mound.

4. Discussion

4.1. Shallow Sediment Carbon

Shallow sediment carbon cycling in Atwater Valley was investigated assuming marine phytodetritus and AOM carbon fixation are the primary sources to SOC and DOC. The difference in $\Delta^{14}C_{SOC}$ values between cores on- and off-mound is likely a result of AOM incorporation of isotopically-depleted DIC into OC [11,12,37], with a substantially greater CH_4 influence on-mound (Figures 2 and 3). There is a pronounced ^{14}C-depletion in SOC on-mound (−955‰ to −890‰) with a slightly more modern signature in surface sediments. Elevation in $\Delta^{14}C$ observed in on-mound (C8) surface sediment results from more modern seawater DIC fixation during AOM, further discussed below. Note that on mound $\delta^{13}C_{DIC}$ was relatively uniform near 0‰ (Figure 6b) and represents a deep sourced signature associated with the fluid advection observed in the mound $\delta^{13}C_{CH4}$ (Figure 5b). An alternate interpretation of on-mound aged carbon data could be sediment erosion resulting in uncovering relic SOC. While erosion could contribute to the aged carbon pattern on-mound, elevated $CaCO_3$ concentrations relative to off-mound values indicate active AOM, resulting in over saturated

DIC and subsequent precipitation (Figure 4). In contrast to on-mound data, off-mound SOC was substantially more modern (−678‰ to −283‰, Figure 3) implying a lower contribution of AOM DIC fixation to carbon cycling. Gordon and Goñi [3] reported surface sediment $\Delta^{14}C_{SOC}$ ranging from −309.1‰ to −228.6‰ in the same general sampling area, with water column depths of 365 to 2270 m. In this study, similar $\Delta^{14}C_{SOC}$ on- and off-mound profiles with more ^{14}C-depletion observed on-mound does indicate depleted radiocarbon DIC contribution to carbon cycling (Figures 2 and 3). The near-constant vertical CRA of the sediments sampled in this study, especially off-mound, suggests sediment mixing or rapid deposition, perhaps created by a shelf slump (Figure 3). Subsequent diagenesis of organic matter with different contributions of ^{14}C-depleted CH_4 between core locations is evident with differences in CRA between on-mound and off-mound cores. $\delta^{13}C$ data in this study provides an estimate of the DIC fixation driven by the AOM of deep sourced CH_4 in shallow sediment carbon cycling. Other investigators have shown that Mississippi River particulate organic carbon (POC) changes from a terrigenous ($\delta^{13}C$ = −28‰ to −26‰) to phytoplankton source ($\delta^{13}C$ = −19‰) near the river mouth [1,3,39,40]. In a previous study, POC-$\delta^{13}C$ reported well offshore near Atwater Valley ranged from −22.5‰ to −18.7‰, [41], in the range of phytodetritus [42,43]. For our study off-mound $\delta^{13}C_{SOC}$ values (−20.5‰ at the surface to −23‰ near the core bottom, Figure 4) were characteristic of SOC dominated by phytodetritus. In contrast, on-mound $\delta^{13}C_{SOC}$ ranged from −25.0‰ down core to −28.2‰ near surface, indicating an alternate carbon source.

A common interpretation in ^{13}C-depleted isotope signatures in coastal waters is carbon sourced from terrestrial plants [39]. However, more recent studies show ^{13}C-depleted $\delta^{13}C_{SOC}$ values observed in these sediments likely results from carbon assimilated into bacterial biomass during CH_4 cycling [22,37]. In anoxic sediments bacterial biomass is incorporated and preserved in solid phase sediments [44,45] and through time can constitute a significant portion of the SOC pool [46,47]. While our data indicate SOC is initially derived from marine phytoplankton, once deposited it is subject to diagenesis which includes incorporation of deep sediment CH_4 into solid phase sediment and pore water carbon pools.

Several additional observations pertaining to sediment carbon pools support interpretation of CH_4 contribution to carbon cycling. In the presence of sediment anaerobic CH_4 oxidation DIC oversaturation results in formation of $CaCO_3$ [48,49]. On-mound where ^{13}C depleted SOC was observed, $CaCO_3$ concentrations were 3 to 4 times higher than off-mound (Figure 4c). On-mound and off-mound data also suggest CH_4 contribution to pore water DOC. On-mound core porewater $\delta^{13}C_{DOC}$ values ranged from −27.6‰ to −24.8‰ with ^{13}C-depletion in shallower sediments, though porewater DOC concentrations showed little variation (Figure 7). The shift to lower $\delta^{13}C_{DOC}$ values in shallow on-mound sediments coincided with a decrease in pore water SO_4^{2-} concentrations and apparent AOM [22]. Off-mound porewater DOC concentrations below the SMT were similar to those on-mound and had depleted $\delta^{13}C_{DOC}$ (−26.2‰; Figure 7) indicating a CH_4 contribution to porewater DOC. In off-mound surface sediments above the SMT, porewater DOC concentrations were lower with an increase in $\delta^{13}C_{DOC}$ (−20.1‰) more typical of a marine phytoplankton source. Here it is assumed that DO^{13}C depletion is not a result of diagenesis or selective metabolism during heterotrophic microbial carbon cycling that would result in isotopic fractionation of the total DOC pool [50,51].

4.2. Methane Source and Cycling

Composition and isotopic signatures of gas pocket samples on-mound indicate a microbial CH_4 source with average C_1/C_2 = 11,000 (methane/ethane) and $\delta^{13}C_{CH4(g)}$ = −71.2‰ (Table 2) [8,52–54]. While data interpretation is contingent on piston core depths, there are indications that on-mound CH_4 originates from deep sediment; (1) $\Delta^{14}C_{CH4(g)}$ depletion measured in on-mound (C3) (−961‰) is a value characteristic of CH_4 that originates in from a deep system [55]; and (2) SO_4^{2-} not observed below the SWI in cores C3 and C7 suggests active advection of deep sediment CH_4 to the surface [22]. In contrast, ^{14}C-enrichment indicated by $\Delta^{14}C_{CH4(g)}$ values in on-mound (C8, −903‰, Figure 2) and presence of a shallow SMT (59 cmbsf) suggests modern seawater DIC is being reduced to CH_4 during methanogenesis. A biogenic CH_4 source, absent of higher molecular weight gases and oil products that are present in a thermogenic source [53], presents an opportunity to study deep sediment CH_4 contribution to shallow sediment carbon cycling. On mound core C3 gas pocket carbon isotope ratios is used as a $CH_{4(g)}$ end-member to estimate CH_4 contribution to organic carbon pools, presented below.

Strong difference in shallow sediment CH_4 cycling was observed within and between cores. Measured on-mound sediment headspace $\delta^{13}C_{CH4}$ values (−70.4‰) deeper than 100 cmbsf were similar to the $\delta^{13}C_{CH4(g)}$ value indicating little microbial CH_4 consumption or production (Figure 5b). In contrast, in the top 100 cm on-mound, sediment headspace $\delta^{13}C_{CH4}$ values were depleted 11‰ relative to $\delta^{13}C_{CH4(g)}$ values (Figure 5, Table 1). The ^{13}C-enrichment indicated by $\delta^{13}C_{CH4(g)}$ values in C8 (−65.8‰) at 240 cmbsf likely results from isotopic fractionation during AOM [22,56]. Where the upward CH_4 flux due to active vertical fluid advection (such as C7 and C3) impedes downward SO_4^{2-} diffusion into sediment, AOM or methanogenesis will not occur and there is not a change in the $\delta^{13}C_{CH4(g)}$ ratio. Depleted $\delta^{13}C_{CH4}$ values on-mound near surface and corresponding enriched $\delta^{13}C_{DIC}$ values do indicate active methanogenesis [57,58]. Methanogenesis typically occurs in marine sediments below AOM [59,60]. However, with advection on-mound, $\delta^{13}C_{DIC}$ data indicate shallow methanogenesis near the SWI (Figure 5b). While enriched $\delta^{13}C_{CH4}$ and an associated SMT was not observed there is potential for seawater SO_4^{2-} to support AOM at the SWI (Figure 5b).

Active CH_4 cycling was also observed in the off-mound core. Above the BSR (Figure 1) there was greater variation in the $\delta^{13}C_{CH4}$ profile with lowest value (−86.9‰), potentially resulting from methanogenesis at a mid-core depth (Figure 5b), just below the SMT (Table 1). Note in a recent study carbon isotope equilibration at the point of sulfate-limited anaerobic oxidation was observed and may account for this depleted $\delta^{13}C_{CH4}$ [61]. Above the SMT, decreased CH_4 concentrations and enriched sediment headspace $\delta^{13}C_{CH4}$ values up to −48.8‰ result from AOM through the SO_4^{2-} gradient (Figure 5). A corresponding depletion in $\delta^{13}C_{DIC}$ values to −47.1‰ (330 cmbsf) and a subsequent increase to −10.5‰ towards the core base (Figure 6) is characteristic of AOM through the SMT located above the zone of methanogenesis [57,62].

4.3. Estimation of CH_4 Contribution to the Shallow Organic Carbon

The relative contributions of phytodetritus and AOM to shallow sediment carbon cycling on-mound and off-mound can be estimate using a simple carbon budget calculation (Equation (5)). We assume sediment CH_4 is primarily oxidized during AOM for energy and DIC is assimilated into cellular

biomass [11–13] with an isotopic fraction of 3.75‰ , a value recently applied in a study on the Hikurangi Margin [37] and an intermediate (2.0‰ to 5.5‰) for isotopic fractionation during DIC assimilation in the reversed tricarboxylic acid cycle [63–65]. For estimating the DIC contribution to SOC during AOM it is assumed $\delta^{13}C_{PD}$ end-member (Equation (5)) was −20.5‰, the off-mound signature in surface sediments with the most modern $\Delta^{14}C_{SOC}$ value (Figure 2). Use of this $\delta^{13}C_{PD}$ end-member is supported by other studies on the TX-LA Shelf where offshore to nearshore sediment $\delta^{13}C$ values ranged from −21.7‰ to −19.7‰ [1,3,40]. On the Gulf of Mexico abyssal plain, with no substantial terrestrial inputs, $\delta^{13}C_{SOC}$ measured values were −20.6‰ [66]. The average porewater $\delta^{13}C_{DIC}$ value measured on-mound, through the SMT (between 34 and 144 cm) was −29.5‰. Adjusting this value for fractionation during DIC fixation (3.75‰, [37]) provides a $\delta^{13}C_{DIC}$ end member of −25.8‰. On-mound, with a $\delta^{13}C_{SOC}$ average of −25.0‰, results in an AOM-DIC contribution to SOC of 85% (Equation (5), Figure 8). We assume, with on-mound advection, AOM occurs at the sediment water column interface where SO_4^{2-} is available and this signature is buried through time. This observation of high CH_4 contribution to shallow sediment carbon cycling is supported with a comparison of regional sedimentation rates and on-mound vertical CH_4 flux. Phytodetritus contribution to SOC in this region is estimated on the basis of a sedimentation rate near this location of 0.005 cm·year^{-1} [1], sediment density of 2.6 gm·cm^{-3} [67], and SOC mineralization of shallow off-mound sediment relative to deep on-mound sediment of 37% [22,68] to be 40.8 mM·C·m^{-2}·year^{-1}. This suggests a small contribution of carbon relative to CH_4 at 3250 mM·C·m^{-2}·year^{-1} (Table 1). Applying this approach to off-mound sediment $\delta^{13}C_{SOC}$ values below 35 cmbsf averaged −22.7‰ and results in a 42% contribution of AOM-derived DIC incorporation to SOC (Figure 8).

Porewater DOC concentrations and $\delta^{13}C_{DOC}$ also indicate different carbon sources between on- and off-mound cores (Figure 7). In this analysis we do assume that porewater bacterial production, cell DOC excretion, and degradation of SOC contribute to porewater DOC. Assuming DIC is fixed into bacterial carbon and subsequently cycled to DOC (Figure 8), the contribution of AOM to DOC (Equation (5)) can be estimated using the phytodetritus end-member $\delta^{13}C_{PD}$ of −20.5‰ and $\delta^{13}C_{DIC}$ of −25.8‰. The $\delta^{13}C_{DOC}$ average off-mound (−24.3‰), suggests 72% of DOC below the SMT is AOM derived (Figure 8). The on-mound average $\delta^{13}C_{DOC}$ value of −25.6‰ through the entire C7 core indicates an indirect contribution of AOM to porewater DOC of 96%. The production of DOC via AOM in sediment may result in significant contribution relative to phytoplankton derived carbon. It is important to note that patterns in $\delta^{13}C_{DIC}$ and $\delta^{13}C_{DOC}$ depletion were similar in the vertical core profiles and with high porewater DOC concentrations ogranoclastic degradation of DOC and subsequent production from light DIC from further AOM can result in an overestimate of AOM related DOC production. Furthermore acetogenesis can contribute to the observation of depleted ^{13}C in the DOC [69]. Also, it is interesting that this observation is similar to a recent study off the coast of New Zealand where AOM contribution to porewater DOC was estimated to be up to 71% at a location with lower vertical CH_4 flux rates [37].

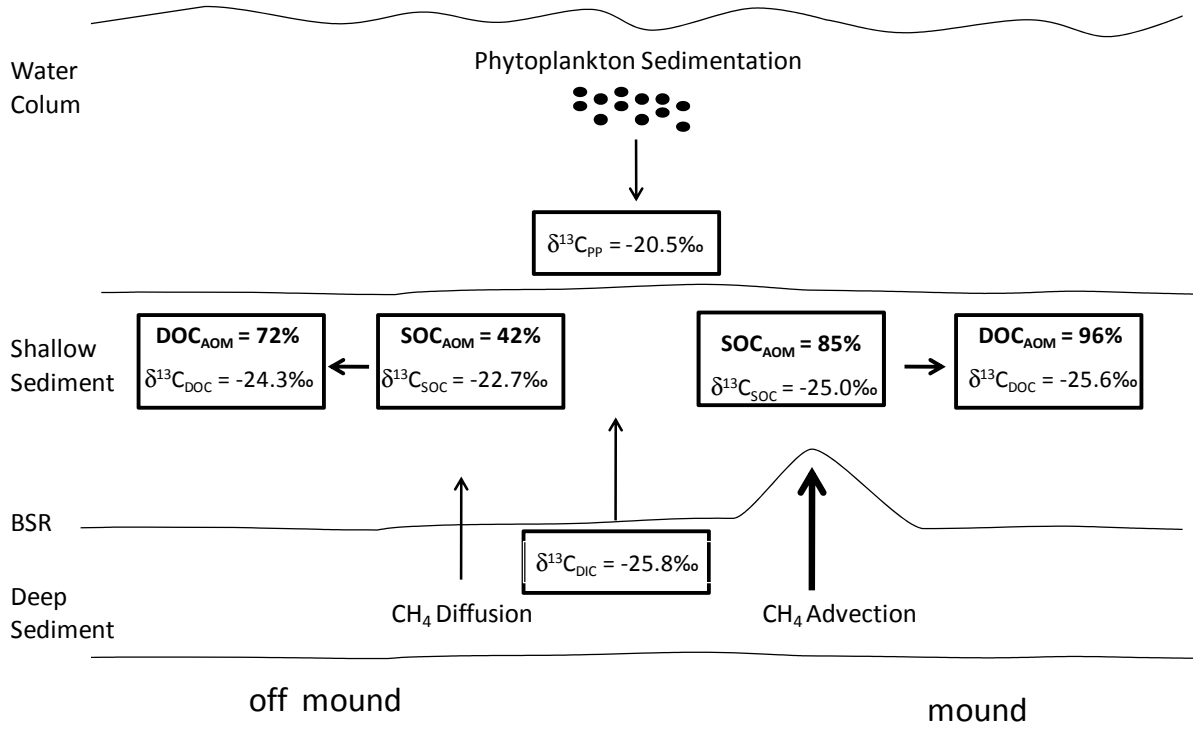

Figure 8. A summary of dissolved organic carbon (DIC) and phytoplankton biomass contributions to shallow SOC and DOC at the on-mound and off-mound sites using $\delta^{13}C$ values.

5. Conclusions

Diffusive and advective fluxes of deep sediment CH_4 contribute significantly to shallow sediment carbon cycling in Atwater Valley, Gulf of Mexico. Deep salt diapirs at this study location are predicted to result in destabilization of CH_4 hydrates and result in an elevated vertical methane flux [22,23]. This prediction is supported in the observation of a substantial rise in the BSR (Figure 1c).The upward flux of deep sediment CH_4 via fluid advection on-mound supports a substantial fraction of sediment carbon production (up to 85%), whereas marine phytoplankton sourced carbon contributes ~50% where there is a low diffusive CH_4 flux (Figure 8). Consistent ^{13}C-enriched $\delta^{13}C_{DIC}$ values deeper than 100 cmbsf and the ^{14}C-depleted $\Delta^{14}C_{SOC}$ and $\Delta^{14}C_{CH4}$ values measured in gas pockets on-mound can be interpreted as long-term mound formation driven by active advection that supported shallow sediment carbon cycling driven by AOM near the SWI where SO_4^{2-} is abundant. The cycling of CH_4 via AOM is reflected in the organic and inorganic carbon pools. The variation in CH_4 cycling in an advection dominated on-mound sediment and a diffusion dominated sediment off-mound is evident in the same sediment carbon pools. Observed $\delta^{13}C_{DIC}$ profiles followed changes in $\delta^{13}C_{CH4}$ values, as did $\delta^{13}C_{CaCO3}$ values, indicating oxidation of CH_4 during AOM was occurring in the sediment pore fluids on the mound. Mass balances using $\delta^{13}C$ of CH_4 and SOC showed a large difference in the estimated contribution of deep sediment CH_4 to the shallow sediment carbon pools off and on-mound relative to marine phytoplankton. The DOC pool in sediment porewaters also reflected a significant contribution (up to 96%) from deep sediment CH_4. In another study on the TX-LA Shelf, petroleum seeps were found to contribute 40% to 60% to the total organic C in a shallower slope region [17].

This study suggests a need for global consideration of the distribution of deep sediment CH_4, especially hydrate bound methane, and the flux of carbon from this globally-significant carbon pool to shallow sediments. More estimates of deep sediment CH_4 and petroleum contributions to shallow sediments and the water column will help refine marine carbon cycling models and budget estimates and improve predictions of the impacts of climate change on these reservoirs. The current estimate for the world coastal CH_4 hydrate distribution is 21×10^{15} m^3 of CH_4 at standard temperature and pressure [8]. A more thorough understanding of the potential for fixation of CH_4 into organic carbon and carbonate phases in shallow sediments will assist in evaluating deep sediment sourced CH_4 fluxes through the shallow sediments to the water column and the atmosphere.

Supplementary Materials

Supplementary materials can be accessed at: http://www.mdpi.com/1996-1073/8/3/1561/s1.

Acknowledgments

Warren Wood, NRL-Stennis Space Center, MS provided seismic profiles and seafloor topography. Ross Downer, Milbar Hydo-Test, Inc. (Shreveport, LA, USA) was lead for all coring operations. We appreciate the technical discussions and reviews of this manuscript from Paula Rose, Jeff Chanton, Thomas Boyd, and Leila Hamdan. David Knies contributed to radiocarbon analyses. We also appreciate the support by the crew of the *RV Gyre.* Finally, reviewers of this manuscript have provided excellent input to research and the presentation. This research was supported by Department of Energy-National Energy Technology Laboratory, Office of Naval Research and the US Naval Research Laboratory.

Author Contributions

All authors have contributed to writing and revisions of this manuscript.

Conflicts of Interest

The authors declare no conflict of interest.

References

1. Goñi, M.A.; Ruttenberg, K.C.; Eglington, T.I. A reassesment of the sources and importance of land-derived organic matter in surface sediment from the Gulf of Mexico. *Geochem. Cosmochim. Acta* **1998**, *62*, 3055–3075.
2. Bianchi, T.S.; Mitra, S.; McKee, B.A. Sources of terrestrially-derived organic carbon in lower Mississippi River and Louisiana shelf sediments: Implications for differential sedimentation and transport at the coastal margin. *Mar. Chem.* **2002**, *77*, 211–223.
3. Gordon, E.S.; Goñi, M.A. Controls on the distribution and accumulation of terrigenous organic matter in sediments from the Mississippi and Atchafalaya river margin. *Mar. Chem.* **2004**, *92*, 331–352.

4. Mayer, L.M.; Schick, L.L.; Allison, M.A.; Rutthenberg, K.C.; Bentley, S.J. Marine *vs.* terrigenous organic matter in Louisiana coastal sediments: The uses of bromine organic carbonratios. *Mar. Chem.* **2007**, *107*, 244–254.
5. Rabalais, N.N.; Atilla, N.; Normandeau, C.; Turner, R.E. Ecosystem history of Mississippi River influenced continental shelf revealed through preserved phytoplankton pigments. *Mar. Pollut. Bull.* **2004**, *49*, 537–547.
6. Ruttenberg, K.C.; Goñi, M.A. Phosphourus distribution, C:N:P ratios, and δ^{13}Coc in arctic, temperate, and tropical coastal sediments: Tools for characterizing bulk sedimentary organic matter. *Mar. Geol.* **1997**, *139*, 123–145.
7. Anderson, R.K.; Scalan, R.S.; Parker, P.L.; Behrens, E.W. Seep oil and gas in Gulf of Mexico slope sediment. *Science* **1998**, *222*, 619–621.
8. Milkov, A.V. Molecular and stable isotope compositions of natural gas hydraes: A revised global data set and basic interpretations in the context of geological settings. *Org. Geochem*. **2005**, *36*, 681–702.
9. Borowski, W.S.; Paull, C.K.; Ussler, W., III. Marine porewater sulfate profiles indicate *in situ* methane flux from underlying gas hydrate. *Geology* **1996**, *24*, 655–658.
10. Pancost, R.D.; Damste, J.S.S.; de Lint, S.; van der Maarel, M.J.E.C.; Gottschal, J.C.; the Medinaut Shipboard Scientific Party. Biomarker evidence for widespread anaerobic methane oxidation in Mediterranean sediments by a consortium of methanogenic archaea and bacteria. *Appl. Environ. Microbiol*. **2000**, *66*, 1126–1132.
11. Knittel, K.; Boetius, A. Anaerobic oxidation of methane: Progress with an unknown process. *Annu. Rev. Microbiol*. **2009**, *63*, 311–334.
12. Alperin, M.J.; Hoehler, T.M. Anaerobic methane oxidation by archaea/sulfate-reducing bacteria aggregates: 2. Isotopic constraints. *Am. J. Sci*. **2009**, *309*, 958–984.
13. Wegener, G.; Niemann, H.; Elvert, M.; Hinrichs, K.-U.; Boetius, A. Assimilation of methane and inorganic carbon by microbial communities mediating the anaerobic oxidation of methane. *Environ. Microbiol.* **2008**, *10*, 2287–2298.
14. Kellermann, M.; Wegener, G.; Elvert, M.; Yoshinga, M.Y.; Lin, Y.-S.; Holler, T.; Mollar, X.P.; Knittel, K.; Hinrichs, K.-U. Autotrophy as a predominant mode of carbon fixation in anaerobic methane-oxidizing mincrobial communities. *PNAS* **2012**, *109*, 19321–19326.
15. Leak, D.J.; Dalton, H. Growth yields of methanotrophs. *Appl. Microbiol. Biotechnol*. **1986**, *23*, 470–476.
16. Kelley, C.A.; Coffin, R.B.; Cifuentes, L.A. Stable isotope evidence for alternate carbon sources in the Gulf of Mexico. *Limnol. Oceanogr*. **1998**, *43*, 1962–1969.
17. Wang, X.-C.; Chen, R.F.; Whelan, J.; Eglinton, T. Contribution of "old" carbon from natural marine hydrocarbon seeps to sedimentary and dissolved organic carbon pools in the Gulf of Mexico. *Geophys. Res. Lett*. **2001**, *28*, 3313–3316.
18. Joye, S.B.; Boetius, A.; Orcutt, B.N.; Montoya, R.P.; Schulz, H.N.; Ericson, M.J.; Lugo, S.K. The anaerobic oxidation of methane and sulfate reduction in sediments from Gulf of Mexico cold seeps. *Chem. Geo.* **2004**, *205*, 219–238.
19. Paull, C.K.; Ussler, W., III; Lorenson, T.; Winters, W.; Dougherty, J. Geochemical constraints on the distribution of gas hydrates in the Gulf of Mexico. *Geo. Mar. Lett*. **2005**, *25*, 273–280.

20. Ruppel, C.; Dickens, G.R.; Castellini, D.G.; Gilhooly, W.; Lisarralde, D. Heat and salt inhibition of gas hydrae formation in the northern Gulf of Mexico. *Geophys. Res. Lett*. **2005**, *3*, L04605, doi:1029/2004GL021909.
21. Lapham, L.L.; Chanton, J.P.; Martens, C.S.; Sleeper, S.; Woolsey, J.R. Microbial activity in surficial sediments overlying acoustic wipeout zones at a Gulf of Mexico cold seep. *Geochem. Geophys. Geosyst.* **2008**, *9*, doi:10.1029/2008GC001944.
22. Coffin, R.B.; Hamdan, L.; Plummer, R.; Smith, J.; Gardner, J.; Wood, W.T. Analysis of methane and sulfate flux in methane charged sediments from the Mississippi Canyon, Gulf of Mexico. *Mar. Pet. Geol*. **2008**, *25*, 977–987.
23. Wood, W.T.; Hart, P.E.; Hutchinson, D.R.; Dutta, N.; Snyder, F.; Coffin, R.B.; Gettrust, J.F. Gas and gas hydrate distribution around seafloor seeps in Mississippi Canyon, Northern Gulf of Mexico, using multi-resolution seismic imagery. *Mar. Pet. Geol.* **2008**, *9*, 952–959.
24. Weimer, P.; Buffler, R.T. Structural geology and evolution of the Mississippi fan fold belt, deep Gulf of Mexico. *AAPG Bull*. **1992**, *76*, 225–251.
25. Goodwin, R.H.; Prior, D.B. Geometry and depositional sequences of the Mississippi Canyon, Gulf of Mexico. *J. Sediment. Res*. **1989**, *59*, 318–329.
26. Ellwood, B.B.; Balsam, W.L.; Roberts, H.H. Gulf of Mexico sediment sources and sediment transport trends from magnetic susceptibility measurements of surface samples. *Mar. Geol*. **2006**, *230*, 237–248.
27. Coffin, R.B.; Gardner, J.; Pohlman, J.; Downer, R.; Wood, W. *Methane Hydrate Exploration, Atwater Valley, Texas-Louisiana Shelf: Geophysical And Geochemical Profiles*; Naval Research Laboratory: Washington, DC, USA, 2006.
28. Reeburgh, W.S. An improved interstitial water sampler. *Limnol. Oceanogr.* **1967**, *12*, 163–165.
29. Plummer, R.E.; Pohlman, J.; Coffin, R.B. *Compound-Specific Stable Carbon Isotope Analysis of Low-Concentration Complex Hydrocarbon Mixtures from Natural Gas Hydrate Systems*; American Geophysical Union: Washington, DC, USA, 2005.
30. Osburn, C.L.; St-Jean, G. The use of wet chemical oxidation with high-amplification isotope ratio mass spectrometry (WCO-IRMS) to measure stable isotope values of dissolved organic carbon in seawater. *Limnol. Oceanogr. Methods* **2007**, *5*, 296–308.
31. Pohlman, J.W.; Knies, D.L.; Grabowski, K.S.; DeTurck, T.M.; Treacy, D.J.; Coffin, R.B. Sample distillation/graphitization system for carbon pool analysis by accelerator mass spectrometry (AMS). *Nucl. Instrum. Methods Phys. Res. Sect. B Beam Interact. Mater. Atoms* **2000**, *172*, 428–433.
32. Grabowski, K.S.; Knies, D.L.; DeTurck, T.M.; Treacy, D.J.; Pohlman, J.W.; Coffin, R.B.; Hubler, G.K. A report on the Naval Research Laboratory AMS facility. *Nucl. Instrum. Methods Phys. Res. Sect. B Beam Interact. Mater. Atoms* **2000**, *172*, 34–39.
33. Tumey, S.T.; Grabowski, K.S.; Knies, D.L.; Mignerey, A.C. Data collection, filtering and analysis at the Naval Research Laboratory trace element accelerator mass spectrometry facility. *Nucl. Instrum. Methods Phys. Res. Sect. B Beam Interact. Mater. Atoms* **2004**, *176*, 428–433.
34. Stuiver, M.; Polach, H.A. Discussion: Reporting of ^{14}C data. *Radiocarbon* **1977**, *19*, 355–363.
35. Stuiver, M. International agreements and the use of the new oxalic acid standard. *Radiocarbon* **1983**, *25*, 793–795.

36. Donahue, D.J.; Linick, T.W.; Jull, A.J.T. Isotope-ratio and background corrections for accelerator mass spectrometry radiocarbon measurements. *Radiocarbon* **1990**, *32*, 135–142.
37. Coffin, R.B.; Hamdan, L.J.; Smith, J.P.; Rose, P.S.; Plummer, R.E.; Yoza, B.; Pecher, I.; Montgomery, M.T. Contribution of vertical methane flux to shallow sediment carbon pools across porangahau ridge, New Zealand. *Energies* **2014**, *7*, 5332–5356, doi:10.3390/en7085332.
38. Macko, S.A.; Ostrom, N.E. Pollution studies using stable isotopes. In *Stable Isotopes in Ecology and Environmental Science*; Lajtha, K., Michener, R., Eds.; Blackwell Scientific Publications: Hoboken, NJ, USA, 1994; pp. 45–62.
39. Fry, B. Using stable isotopes to monitor watershed influences on aquatic trophodynamics. *Can. J. Fish. Aquat. Sci.* **1999**, *56*, 2167–2171.
40. Gordon, E.S.; Goñi, M.A. Source and distribution of terrigenous organic matter delivered by the Atchafalaya River to sediments in the northern Gulf of Mexico. *Geochem. Cosmochim. Acta* **2003**, *67*, 2359–2375.
41. Wang, X.; Chen, R.F.; Gardner, G.B. Sources and transport of dissolved and particulate organic carbon in the Mississippi River estuary and adjacent coastal waters of the northern Gulf of Mexico. *Mar. Chem.* **2004**, *89*, 241–256.
42. Peterson, B.J.; Howarth, R.W.; Garritt, R.H. Multiple stable isotopes used to trace the flow of organic matter in estuarine food webs. *Science* **1985**, *277*, 1361–1363.
43. Chen, X.; Lohrenz, S.E.; Wiesenburg, D.A. Distribution and controlling mechanisms of primary production on the Louisianan-Texas continental shelf. *J. Mar. Syst.* **2000**, *25*, 179–207.
44. Burdige, D.J.; Martens, C.S. Biogeochemical cycling in an organic-rich coastal marine basin: The sedimentary cycling of dissolved, free amino acids. *Geochim. Cosmochim. Acta* **1990**, *54*, 3033–3052.
45. Lee, C. Controls on organic carbon preservation: The use of stratified water bodies to compare intrinsic rates of decomposition in oxic and anoxic systems. *Geochim. Cosmochim. Acta* **1992**, *56*, 3323–3335.
46. Canuel, E.A.; Martens, C.S. Seasonal variations in the sources and alteration of organic matter associated with recently-deposited sediments. *Org. Geochem*. **1993**, *20*, 563–577.
47. Gong, C.; Hollander, D.J. Differential contribution of bacteria to sedimentary organic matter in oxic and anoxic environments, Santa Monica Basin, California. *Org. Geochem*. **1997**, *26*, 545–563.
48. Orphan, V.J.; Hinrichs, K.U.; Ussler, W., III; Paull, C.K.; Taylor, L.T.; Sylva, S.P.; Hayes, J.M.; Delong, E.F. Comparative analysis of methane-oxidizing archaea and sulfate-reducing bacteria in anoxic marine sediments. *Appl. Environ. Microbiol*. **2001**, *67*, 1922–1934.
49. Reeburgh, W.S. Oceanic methane biogeochemistry. *Chem. Rev*. **2007**, *107*, 486–513.
50. Goevert, D.; Conrad, R. Effect of substrate concentration on carbon isotope fractionation during acetoclastic methanogenesis by *Methanosarcina barkeri* and *M. acetivorans* and in rice field soil. *Appl. Environ. Microbiol*. **2009**, *75*, 2605–2612.
51. Szynkiewicz, A.M.; Jedrysek, O.; Kurasiewicz, M. Carbon isotope effects during precipitation of barium carbonate: Implications for environmental studies. *Environ. Chem. Lett*. **2006**, *4*, 29–35.
52. Martens, C.S.; Chanton, J.P.; Paull, C.K. Fossil biogenic methane at the Florida escarpment. *Geology* **1991**, *19*, 851–854.

53. Sassen, R.; MacDonald, I.R. Hydrocarbons of experimental and natural gas hydrates, Gulf of Mexico continental slope. *Org. Geochem.* **1997**, *26*, 289–293.
54. Sassen, R.; Sweet, S.T.; DeFreitas, D.A.; Morelos, J.A.; Milkov, A.V. Gas hydrate and crude oil from the Mississippi Fan Foldbelt, downdip Gulf of Mexico Salt Basin: Significance to petroleum system. *Org. Geochem*. **2001**, *32*, 999–1008.
55. Pohlman, J.W.; Kaneko, M.; Heuer, V.B.; Coffin, R.B.; Whiticar, M. Methane soucrces and production in the north Cascadia Margin gas hydrate system. *Earth Planet. Sci. Lett*. **2009**, *287*, 504–512.
56. Whiticar, M.J. Carbon and hydrogen isotope systematics of bacterial formation and oxidation of methane. *Chem. Geol.* **1999**, *16*, 291–314.
57. Boetius, A.; Ravenschlag, K.; Schubert, C.J.; Rickert, D.; Widdel, F.; Gleske, A.; Amann, R.; Jørgensen, B.B.; Witte, U.; Pfannkuche, O. A marine microbial consortium apparently mediating anaerobic oxidation of methane. *Nature* **2000**, *407*, 623–626.
58. Orphan, V.J.; House, C.H.; Hinrichs, K.-U.; McKeegan, K.D.; DeLong, E.F. Methane-consuming archea revealed by directly coupled isotopic and phylogenetic analysis. *Science* **2001**, *293*, 484–487.
59. Alperin, M.J.; Blair, N.E.; Albert, D.B.; Hoehler, T.M.; Martens, C.S. Factors that control the stable carbon isotopic composition of methane produced in an anoxic marine sediment. *Glob. Biogeochem. Cycles* **1992**, *6*, 271–291.
60. Hoehler, T.M.; Alperin, M.J.; Albert, D.B.; Martens, C.S. Field and laboratory studies of methane oxidation in an anoxic marine sediment: Evidence for a methanogen-sulfate reducer consortium. *Glob. Biogeochem. Cycles* **1994**, *8*, 451–463.
61. Yoshinaga, M.Y.; Holler, T.; Goldhammer, T.; Wegener, G.; Pohlman, J.W.; Brunner, B.; Kuypers, M.M.M.; Hinrichs, K-U.; Elvert, M. Carbon isotope equilibration during sulphate-limited anaerobic oxidation of methane. *Nat. Geosci.* **2014**, *7*, doi:10.1038/NGEO2069.
62. Borowski, W.S.; Paull, C.K.; Ussler, W., III. Global and local variations of interstitial sulfate gradients in the deep-water, continental margin sediments: Sensitivity to underlying methane and gas hydrates. *Mar. Geol.* **1999**, *159*, 131–154.
63. House, C.H.; Schopf, J.W.; Stetter, K.O. Carbon isotopic fractionation by Archaens and other thermophilic prokaryotes. *Org. Geochem.* **2003**, *34*, 345–356.
64. Zhang, C.L.; Fouke, B.W.; Bonheyo, G.T.; Peackock, A.D.; White, D.C.; Huang, Y.; Romanek, C.S. Lipid biomarkers and carbon-isotopes of modern travertine deposits (Yellowstone Natioinal Park, USA): Implications for biogeochemical dynamics in hot-spring systems. *Geochem. Cosmochim. Acta* **2004**, *68*, 3157–3169.
65. Quandt, L.; Gottschalk, G.; Ziegler, H.; Stichler, W. Isotope discrimination by photosynthetic bacteria. *REMS Microbiol. Lett.* **1977**, *1*, 125–128.
66. Morse, J.W.; Beazley, M.J. Organic matter in deepwater sediments of the Northern Gulf of Mexico and its relationship to the distribution of benthic organisms. *Deep Sea Res. II* **2008**, *55*, 2563–2571.
67. Burdige, D.J. *Geochemistry of Marine Sediments*; Princeton University Press: Princeton, NJ, USA, 2006.

68. Martens, C.S.; Klump, J.V. Biogeochemical cycling of an organic-rich coastal marine basin 4. An organic carbon budget for sediments dominated by sulfate reduction and methanogenesis. *Geochem. Cosmochim. Acta* **1984**, *48*, 1987–2004.
69. Hoehler, T.M.; Albert, D.B.; Alperin, M.J.; Martens, C.S. Acetogenesis from CO_2 in an anoxic marine sediment. *Limnol. Oceanogr.* **1999**, *44*, 662–667.